

- 28098 (1994); M. L. Whitelaw, J.-A. Gustafsson, L. Poellinger, *Mol. Cell. Biol.* **14**, 8343 (1994).
3. A. B. Okey, D. S. Riddick, P. A. Harper, *Trends Pharmacol. Sci.* **15**, 226 (1994).
  4. G. W. Lucier, C. J. Portier, M. A. Gallo, *Environ. Health Perspect.* **101**, 36 (1993); M. J. DeVito, X. Ma, J. G. Babish, M. Menache, L. Birnbaum, *Toxicol. Appl. Pharmacol.* **124**, 82 (1994); H. Huoskonen, M. Unkila, R. Pohjanvirta, J. Tuomisto, *ibid.*, p. 174; P. A. Bertazzi *et al.*, *Epidemiology* **4**, 398 (1993); L. S. Birnbaum, *Environ. Health Perspect.* **102**, 676 (1994).
  5. D. J. McConkey, P. Hartzell, S. K. Duddy, H. Hakansson, S. Orrenius, *Science* **242**, 256 (1988).
  6. D. W. Nebert, *CRC Crit. Rev. Toxicol.* **20**, 153 (1989).
  7. \_\_\_\_\_, D. D. Peterson, A. Puga, *Pharmacogenetics* **1**, 68 (1991).
  8. W. Li, S. Donat, O. Dohr, K. Unfried, J. Abel, *Arch. Biochem. Biophys.* **315**, 279 (1994).
  9. K. M. Dolwick *et al.*, *Mol. Pharmacol.* **44**, 911 (1993).
  10. S. Kimura, F. J. Gonzalez, D. W. Nebert, *Mol. Cell. Biol.* **6**, 1471 (1986).
  11. F. J. Gonzalez and D. W. Nebert, *Nucleic Acids Res.* **13**, 7269 (1985).
  12. U. Savas *et al.*, *J. Biol. Chem.* **269**, 14905 (1994); T. R. Sutter *et al.*, *ibid.*, p. 13092; Z. Shen *et al.*, *DNA Cell Biol.* **13**, 763 (1994).
  13. T. R. Sutter, K. Guzman, K. M. Dold, W. F. Greenlee, *Science* **254**, 415 (1991); A. Puga, D. W. Nebert, F. Carrier, *DNA Cell Biol.* **11**, 269 (1992).
  14. B. D. Abbott, G. H. Perdew, L. S. Birnbaum, *Toxicol. Appl. Pharmacol.* **126**, 16 (1994); D. W. Nebert, *Biochem. Pharmacol.* **47**, 25 (1994).
  15. M. Capecchi, *Science* **244**, 1288 (1989).
  16. S. L. Mansour *et al.*, *Nature* **336**, 348 (1988).
  17. F. J. Gonzalez, *Pharmacol. Rev.* **40**, 243 (1989); R. W. Robertson, L. Zhang, D. S. Pasco, J. B. Fagan, *Nucleic Acids Res.* **22**, 1741 (1994); J. O. Miners and P. I. Mackenzie, *Pharmacol. Ther.* **51**, 347 (1991).
  18. F. J. Gonzalez and D. W. Nebert, *Trends Genet.* **6**, 182 (1990).
  19. S. Hayashi *et al.*, *Carcinogenesis* **15**, 801 (1994).
  20. A. Poland and J. C. Knutson, *Annu. Rev. Pharmacol. Toxicol.* **22**, 517 (1982).
  21. To inactivate the *Ahr* gene in ES cells, we isolated a genomic clone from a 129/SV mouse library (Stratagene) with a 96-nucleotide oligomer complementary to the 5' coding region of the murine AHR complementary DNA [nucleotides 978 to 1073 in M. Ema *et al.*, *Biochem. Biophys. Res. Commun.* **184**, 246 (1992)]. A 7.5-kb fragment containing exon 1 from this genomic clone was digested with Sal I (phage vector cloning site) and Bam HI, and cloned into the vector pMC-TK (negative selection marker conferred by the HSV-TK cassette). To generate the replacement targeting construct, we deleted the coding exon 1 by digestion with Nar I and insertion of a modified *neo*-poly(A) cassette (positive selection marker that confers resistance to G418) with compatible Cla I ends. The final construct in pUC9 was linearized at a unique Xho I site and introduced by electroporation into  $1 \times 10^7$  ES cells with a Bio-Rad Gene Pulser (250 V, 250  $\mu$ F). Electroporated ES cells were plated onto a monolayer of  $\gamma$ -irradiated, neomycin-resistant mouse primary fibroblasts and the cells were grown in the presence of leukemia inhibitor factor (1000 U/ml) (Gibco BRL). Selection was performed for 7 to 8 days with G418 (350  $\mu$ g/ml) and 5  $\mu$ M ganciclovir. Surviving clones were isolated and analyzed for the homologous recombination event.
  22. Genomic DNA was digested with Xba I or Hind III and subjected to electrophoresis on 0.7 and 0.45% agarose gels, respectively. The gels were blotted under alkaline conditions with Gene Screen Plus nylon membranes (DuPont), which were then hybridized at 42°C in 10% dextran sulfate—50% formamide solution with random primer-labeled genomic DNA probe or neomycin cassette at a radioactive concentration of  $1.5 \times 10^6$  cpm/ml. The membranes were washed at 65°C for 30 min in  $2 \times$  standard saline citrate (SSC) containing 0.5% SDS and then for 15 min in  $1 \times$  SSC containing 0.5% SDS.
  23. Animals were administered a single intraperitoneal injection (25  $\mu$ l) of TCDD (Accu-Standard) dissolved in 1,4-dioxane (Baxter) at a dose of 40  $\mu$ g per kilo-

gram of body mass. Control animals were injected with the same volume of pure solvent. Mice were killed by carbon monoxide asphyxiation 20 hours after injection. The organs were removed rapidly, weighed, and stored in liquid nitrogen until use. TCDD was of the highest purity commercially available (>99%) and 1,4-dioxane was of high performance liquid chromatography quality.

24. Total liver RNA was isolated from the frozen tissues according to the guanidinium-thiocyanate method [P. Chomczynski and N. Sacchi, *Anal. Biochem.* **162**, 156 (1987)] and 15  $\mu$ g were applied to 1% agarose-formaldehyde gels. The gels were blotted onto Gene Screen Plus nylon membranes, which were then hybridized at 42°C in 10% dextran sulfate—50% formamide solution containing the appropriate murine complementary DNA probes. The membranes were washed at 65°C for 30 min in  $2 \times$  SSC containing

0.5% SDS and then for 20 min in  $0.5 \times$  SSC containing 0.5% SDS. Quantitation of the amounts of mRNA was performed by exposing blots to Phosphor Screens (Eastman-Kodak) for 24 hours. The screens were then analyzed with a Phosphorimager (Molecular Dynamics) and the signals were quantified by volume integration with software provided by the manufacturer.

25. D. M. Hilbert, K. L. Holmes, A. O. Anderson, S. Rudikoff, *Eur. J. Immunol.* **23**, 2412 (1993).
26. We thank U. Hochgeschwender for the J1 cells, which were originally provided by R. Jaenisch, and for technical support; D. Accili for helpful suggestions; and G. Miller, E. Lee, and H. Westphal for technical assistance. Supported in part by NIH grants R01 ES06811 and P30 ES06096 to D.W.N.

14 December 1994; accepted 24 February 1995

## Inhibition of Proteasome Activities and Subunit-Specific Amino-Terminal Threonine Modification by Lactacystin

Gabriel Fenteany, Robert F. Standaert, William S. Lane, Soongyu Choi, E. J. Corey, Stuart L. Schreiber\*

Lactacystin is a *Streptomyces* metabolite that inhibits cell cycle progression and induces neurite outgrowth in a murine neuroblastoma cell line. Tritium-labeled lactacystin was used to identify the 20S proteasome as its specific cellular target. Three distinct peptidase activities of this enzyme complex (trypsin-like, chymotrypsin-like, and peptidylglutamyl-peptide hydrolyzing activities) were inhibited by lactacystin, the first two irreversibly and all at different rates. None of five other proteases were inhibited, and the ability of lactacystin analogs to inhibit cell cycle progression and induce neurite outgrowth correlated with their ability to inhibit the proteasome. Lactacystin appears to modify covalently the highly conserved amino-terminal threonine of the mammalian proteasome subunit X (also called MB1), a close homolog of the LMP7 proteasome subunit encoded by the major histocompatibility complex. This threonine residue may therefore have a catalytic role, and subunit X/MB1 may be a core component of an amino-terminal-threonine protease activity of the proteasome.

Lactacystin (compound **2** in Fig. 1) was discovered on the basis of its ability to induce neurite outgrowth in the murine neuroblastoma cell line Neuro-2a (1). Lactacystin also inhibits proliferation of other cell types, suggesting that its target is not exclusive to Neuro-2a cells (2). To understand the cellular effects of lactacystin, we tested a series of analogs and found that a synthetic  $\beta$ -lactone (compound **1** in Fig. 1) related to lactacystin showed similar biological activity, whereas the corresponding acid, formally the product of hydrolysis of the lactacystin thioester or the  $\beta$ -lactone, did not (2). These and other data suggested that an electrophilic carbonyl at C4 was essential for the biological activity of lacta-

cystin, and thus that its target might be an enzyme containing a catalytic nucleophile, such as a protease or a lipase (2). The C4 carbonyls of both the thioester and the  $\beta$ -lactone are reactive electrophiles, whereas the carboxylate of the dihydroxy acid is essentially inert to nucleophilic attack.

To purify and identify the target, we synthesized [ $^3$ H]lactacystin and the [ $^3$ H] $\beta$ -lactone at a specific activity of 3.4 Ci/mmol (Fig. 1). Incubation of crude extracts from Neuro-2a cells or bovine brain with [ $^3$ H]lactacystin (or [ $^3$ H] $\beta$ -lactone), followed by SDS-polyacrylamide gel electrophoresis (SDS-PAGE) and fluorography, revealed the presence of an intensely labeled protein band of ~24 kD (Fig. 2) and a weakly labeled band at ~32 kD. The latter is not evident in Fig. 2 and appeared only with prolonged exposure times, but the 24-kD band was visibly radiolabeled even after a 5-min treatment with 1  $\mu$ M [ $^3$ H] $\beta$ -lactone or [ $^3$ H]lactacystin (3). Similar results were obtained with extracts from *Saccharomyces cerevisiae* and bovine liver and thymus. La-

G. Fenteany, R. F. Standaert, S. L. Schreiber, Howard Hughes Medical Institute, Departments of Chemistry and Molecular and Cellular Biology, Harvard University, Cambridge, MA 02138, USA.

W. S. Lane, Harvard Microchemistry Facility, Harvard University, Cambridge, MA 02138, USA.

S. Choi and E. J. Corey, Department of Chemistry, Harvard University, Cambridge, MA 02138, USA.

\*To whom correspondence should be addressed.

being by [ $^3\text{H}$ ]lactacystin (or [ $^3\text{H}$ ] $\beta$ -lactone) was completely prevented by the simultaneous addition of an excess of unlabeled lactacystin,  $\beta$ -lactone, or other biologically active analogs, but not by the addition of dihydroxy acid or other biologically inactive analogs (Fig. 2) (2, 3). These results suggest that the interaction is saturable, specific, and relevant to the cellular effects of lactacystin.

The lactacystin-binding proteins were purified from bovine brain (4), on the basis of labeling by [ $^3\text{H}$ ]lactacystin or [ $^3\text{H}$ ] $\beta$ -lactone, and gel filtration chromatography revealed that both reside in the same high-molecular weight protein complex. Treatment with [ $^3\text{H}$ ]lactacystin or [ $^3\text{H}$ ] $\beta$ -lactone did not dissociate the complex, and the bound radioactivity uniquely comigrated with it. The mass of the purified complex was  $\sim 700$  kD, and SDS-PAGE showed that it consisted of numerous proteins with masses of approximately 24 to 32 kD. Edman degradation revealed the sequences of

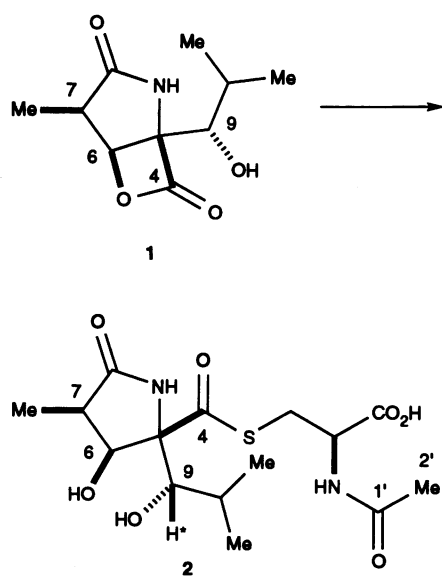


**Fig. 1.** Synthesis of [ $^3\text{H}$ ]lactacystin. Lactacystin **2** was prepared from the related  $\beta$ -lactone **1**, which was tritiated by an oxidation-reduction sequence. Unlabeled **1** was oxidized at C9 to the ketone with the Dess-Martin periodinane (DMP) (76%) (31) in dichloromethane and then reduced with [ $^3\text{H}$ ]NaBH $_4$  (NEN, 13.5 Ci/mmol) in 1,2-dimethoxyethane/1% H $_2$ O at 22°C for 10 min to afford tritiated **1** along with its C9-epimer (2:3 ratio). The isomeric  $\beta$ -lactones were separated by HPLC (Rainin Microsorb SiO $_2$  column, 4.5 mm by 100 mm, 10% *i*-Pr-OH in hexane) and reacted with *N*-acetylcysteine (0.5 M) and triethylamine (1.5 M) in CH $_3$ CN at 22°C for 1 hour to afford lactacystin (9S) **2** (specific activity = 3.4 Ci/mmol) and its C9-epimer (9R), which were purified from their respective reaction mixtures by reversed-phase HPLC [TSK-Gel ODS-80T $_m$  column (Toso Haas, Philadelphia), 4.6 mm by 250 mm, 10% CH $_3$ CN/0.1% CF $_3$ CO $_2$ H in H $_2$ O]. Me, methyl. The asterisk indicates the radiolabeled atom.

several proteasome subunits in the 24-kD band, which led to a tentative identification of the complex as the 20S proteasome. We treated the complex with [ $^3\text{H}$ ] $\beta$ -lactone or [ $^3\text{H}$ ]lactacystin and subjected it to reversed-phase high-performance liquid chromatography (rpHPLC) to separate the proteasome subunits. Eleven distinct peaks were resolved, but the bound radioactivity was associated exclusively with the first two peaks, and predominantly with the second (Fig. 3), which was labeled much faster than the first (5); the incorporation of radioactivity was prevented by simultaneous addition of excess unlabeled compound. After 2-hour incubation with 10  $\mu\text{M}$  [ $^3\text{H}$ ] $\beta$ -lactone under the conditions described in Fig. 3, there was only trace labeling of the first peak, unlike what was observed after 24 hours (Fig. 3), even though the second peak was saturated with label after 2 hours (3). The first two peaks were judged to be homogeneous by silver staining of SDS-polyacrylamide gels and by sequencing of tryptic fragments, whereas some of the later-eluting, larger peaks were clearly not homogeneous. We estimate that 2 mol of lactacystin or  $\beta$ -lactone bind to 1 mol of the primary lactacystin-binding protein (the second eluted peak) after a 24-hour radiolabeling on the basis of integrated absorbance at 210 nm [and using the standard value of 20.5 as the absorbance (210 nm) for a solution containing 1 mg of protein per milliliter] and on integrated radioactivity from the peak on HPLC chromatograms.

Analysis by SDS-PAGE followed by silver-staining revealed that the first peak to elute from the rpHPLC column contained only a 32-kD protein, corresponding to the weakly labeled 32-kD protein observed in

crude extracts. Sequencing of this secondary lactacystin-binding protein showed it to be the proteasome  $\alpha$  chain (Fig. 4B), a  $\sim 30$ -kD protein identified in purified human erythrocyte proteasome (6) and rat liver proteasome (7) for which only NH $_2$ -terminal sequences exist. It is also a homolog of the *S. cerevisiae* PUP1 proteasome subunit (8). The second peak to elute from the column contained only a 24-kD protein, the primary lactacystin-binding protein. The sequence from the NH $_2$ -terminus of this protein and from derived tryptic fragments showed that 59 of 62 residues were identical to the recently discovered human 20S proteasome subunit X (9), also known as MB1 (10), a reciprocally regulated homolog of the major histocompatibility complex (MHC)-encoded LMP7 proteasome subunit (Fig. 4A).

The 20S proteasome is a large ( $\sim 700$  kD), multicatalytic protease complex that in eukaryotes is composed of about 14 different types of subunits of 21 to 32 kD each [for reviews, see (11)]. In the archaeobacterium *Thermoplasma acidophilum*, the proteasome complex is of a similar size but is composed of only two types of subunits, termed  $\alpha$  and  $\beta$  (12, 13), and the subunits are arranged in a cylindrical stack of four rings in an  $\alpha_7\beta_7\beta_7\alpha_7$  organization (14). Both of the lactacystin-binding proteasome subunits from bovine brain are related to the archaeobacterial proteasome's  $\beta$  subunit. The 20S proteasome in eukaryotes is thought to be structurally similar to the simpler archaeobacterial proteasome but assembles into a larger 26S protease complex that is responsible for the adenosine triphosphate (ATP)-dependent breakdown

**Fig. 2.** Fluorogram of SDS-polyacrylamide gel of crude cell and tissue extracts treated with [ $^3\text{H}$ ]lactacystin with or without unlabeled competitor (added simultaneously) for 24 hours. Lanes 1 and 2 contain crude Neuro-2a extracts ( $\sim 11$   $\mu\text{g}$  total protein per lane), and lanes 3 and 4 contain crude bovine brain extracts ( $\sim 54$   $\mu\text{g}$  total protein per lane). Each extract was treated with 10  $\mu\text{M}$  [ $^3\text{H}$ ]lactacystin with or without 1 mM unlabeled lactacystin; lane 1, no competitor; lane 2, lactacystin; lane 3, no competitor; and lane 4, lactacystin. The positions of molecular size standards and their sizes in kilodaltons are indicated at left. Crude extracts from Neuro-2a cells or bovine brain [in homogenization buffer described in (4)] were incubated with the compounds for 24 hours at room temperature, subjected to SDS-PAGE, stained and destained, treated with EN $^3$ HANCE (NEN) according to the manufacturer's instructions, and dried and exposed to Kodak SB film.

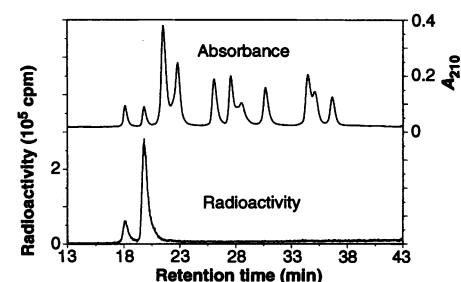


**Fig. 3.** HPLC separation of subunits of proteasome labeled with [ $^3\text{H}$ ] $\beta$ -lactone. Purified 20S proteasome ( $\sim 0.1$   $\mu\text{g}/\mu\text{l}$ ) (4) was incubated at 25°C with 10  $\mu\text{M}$  [ $^3\text{H}$ ] $\beta$ -lactone for 24 hours. Trifluoroacetic acid (TFA) was then added to 0.1% (v/v), and after 20 min, the solution was loaded onto a Vydac C4 column (300  $\text{\AA}$ , 4.6 mm by 150 mm), which had been equilibrated with 20% CH $_3$ CN/H $_2$ O/0.1% TFA, at a flow rate of 0.8 ml/min. The CH $_3$ CN concentration was raised to 40% over 10 min, and then to 55% over 30 min to elute the proteasome subunits. Absorbance was monitored at 210 nm ( $A_{210}$ ), and radioactivity was measured with an in-line flow scintillation detector ( $\beta$ -RAM 2B, IN/US Instruments).

of ubiquitinated proteins [for reviews, see (14)]. Although the 20S proteasome is believed to be the catalytic core of the 26S protease complex, in isolation it does not effect ubiquitin-, ATP-dependent proteolysis. However, the 20S proteasome by itself can cleave certain protein and peptide substrates in an ATP-independent manner. The best characterized of the activities of the 20S proteasome are hydrolysis of the amide bond of small peptides COOH-terminal to hydrophobic, basic, and acidic res-

idues, respectively, termed chymotrypsin-like, trypsin-like, and peptidylglutamyl-peptide hydrolyzing (PGPH) activities. Studies that used group-blocking reagents, inhibitors, and activators, as well as genetic studies in yeast, suggest that the three peptidase activities arise from separate active sites on the proteasome particle. The simpler archaeobacterial proteasome possesses only a chymotrypsin-like specificity (12).

We assessed the effects of lactacystin and the related  $\beta$ -lactone on the activities

of the 20S proteasome, purified to homogeneity (4), using fluorogenic peptide substrates and found that they inhibited all three activities, irreversibly in the case of the chymotrypsin-like and trypsin-like activities and reversibly in the case of the PGPH activity (16). Purified 20S proteasome maintains its activity for several days at room temperature, and in lactacystin- or  $\beta$ -lactone-treated samples inhibition was observed under these conditions for this duration (3). The apparent second-order rate constant for association of the inhibitor with the enzyme,  $k_{\text{assoc}}$ , was determined for each of the activities by assaying for residual activity as a function of time after the addition of inhibitor (Table 1). Lactacystin inhibited the chymotrypsin-like activity the fastest ( $k_{\text{assoc}} = 194 \pm 15 \text{ M}^{-1} \text{ s}^{-1}$ ) and the trypsin-like activity and the PGPH activity at 1/20 and 1/50 of that rate, respectively. That the inhibition rates are different for the three activities further supports the notion that the activities arise from separate active sites. The  $\beta$ -lactone displayed the same rank order of inhibition kinetics but inhibited each activity 15 to 20 times as fast as did lactacystin itself, in accord with the greater chemical reactivity of the  $\beta$ -lactone. It is also possible that upon initial binding the lactacystin thioester is cyclized in a rate-limiting step to the  $\beta$ -lactone, which is then rapidly attacked by the nucleophile.

The inhibition of the proteasome by lactacystin in vivo may prevent the degradation of growth-inhibitory proteins or it may block the proteolytic activation of growth-permissive proteins in the cell. The proteasome is thought to be responsible for the degradation of abnormal and denatured proteins in the cytoplasm and nucleus of the cell, and many regulatory proteins also appear to be degraded by the proteasome as part of the 26S protease complex in a ubiquitin-, ATP-dependent manner [for reviews, see (17)]. The proteasome is also thought to be involved in the processing of antigens for MHC class I presentation [for review, see (18)]. Cyclin degradation has been shown to be required for exit from mitosis (19), and cyclins appear to be degraded by the ubiquitin-proteasome pathway (20). Recently, Palombella *et al.* (21) discovered that the regulated proteolytic processing and activation of the nuclear factor kappa B (NF- $\kappa$ B) p105 precursor protein and the degradation of the inhibitor of NF- $\kappa$ B (I- $\kappa$ B) are mediated by the ubiquitin-proteasome pathway. Lactacystin appears to inhibit the 26S proteasome-mediated, ubiquitin-, ATP-dependent proteolytic processing of the NF- $\kappa$ B precursor protein and the degradation of I- $\kappa$ B (22).

Previously, we showed that lactacystin analogs that cause neurite outgrowth in

**Fig. 4.** Amino acid sequence of purified bovine lactacystin-binding proteins. **(A)** Sequences derived from the ~24-kD primary bovine lactacystin-binding protein from direct NH<sub>2</sub>-terminal sequencing (sequence 1) and tryptic fragments (sequences 2 to 4), aligned with sequences of human proteasome subunit X, predicted from the complementary DNA (cDNA) clone (9), and human LMP7-E2, predicted from the exon 2-containing cDNA clone (26). Sequence 1 (from direct NH<sub>2</sub>-terminal sequencing) is also aligned with sequences of *S. cerevisiae* Pre2, predicted from the genomic clone (27), and *T. acidophilum*  $\beta$  subunit, predicted from the genomic clone (13). The underlined NH<sub>2</sub>-terminal heptapeptide in sequence 1 corresponds to the tryptic fragment that appears to contain a lactacystin-modified NH<sub>2</sub>-terminal threonine residue (boldface). Upper-case letters denote high-confidence sequence, whereas lowercase letters indicate lower confidence assignments. All of the tryptic fragments, including the underlined NH<sub>2</sub>-terminal heptapeptide, were derived from lactacystin-treated 20S proteasome, whereas the direct NH<sub>2</sub>-terminal sequence was obtained from untreated 20S proteasome. **(B)** Sequence derived from the ~32-kD secondary lactacystin-

## A

### Primary bovine lactacystin-binding protein

Sequence 1			
direct NH <sub>2</sub> -terminal sequence			<b>TTTLAFKfRHg</b>
Human subunit X	5	TTTLAFKFRHG	15
Human LMP7-E2	73	TTTLAFKFQHG	83
<i>S. cerevisiae</i> Pre2	76	TTTLAFRFQGG	86
<i>T. acidophilum</i> $\beta$ subunit	9	TTTVGITLKDA	19
Sequence 2			
tryptic fragment		VIEINPYLLGT	MAGGAADcSFwer
Human subunit X	38	VIEINPYLLGT	MAGGAADCSFWER 61
Human LMP7-E2	106	VIEINPYLLGT	MSGCAADCQYWER 129
Sequence 3			
tryptic fragment		GYSYDLEVEEAYDLAR	
Human subunit X	146	GYSYDLEVEQAYDLAR	161
Human LMP7-E2	214	GYRPNLSPEEAYDLGR	229
Sequence 4			
tryptic fragment		DAYSGGVSVSLY	
Human subunit X	171	DAYSGGAVNLYHVR	184
Human LMP7-E2	239	DSYSGGVVNMVYHMK	252

## B

### Secondary bovine lactacystin-binding protein

Tryptic fragments		TTIAGVVYKDGIVLGADTR	
Human erythrocyte proteasome $\alpha$ chain	1	XXIAGVVYKDGIVLGADTR	19
Rat liver proteasome chain 1	1	TTIAGVVYKDG I	12
<i>S. cerevisiae</i> PUP1	30	TTIVGVKFNNGVVIADTR	49

(from lactacystin-treated 20S proteasome) aligned with the NH<sub>2</sub>-terminal sequence of human erythrocyte proteasome  $\alpha$  chain (6), rat liver proteasome chain 1 (7), and *S. cerevisiae* PUP1, the latter predicted from the genomic clone (8). Abbreviations for the amino acid residues are as follows: A, Ala; C, Cys; D, Asp; E, Glu; F, Phe; G, Gly; H, His; I, Ile; K, Lys; L, Leu; M, Met; N, Asn; P, Pro; Q, Gln; R, Arg; S, Ser; T, Thr; V, Val; W, Trp; and Y, Tyr.

Neuro-2a cells also inhibit cell cycle progression in MG-63 human osteosarcoma cells, and that modifications to the  $\gamma$ -lactam part of the molecule impaired both activities whereas modifications to the *N*-acetylcysteine moiety had little or no effect (2). We therefore tested whether the analogs could inhibit the 20S proteasome, focusing on the chymotrypsin-like activity, which is inhibited most rapidly by lactacystin. The same trends found in the biological experiments were apparent in the inhibition studies. The biologically active compounds inhibited the chymotrypsin-like activity, whereas the biologically inactive compounds did not inhibit this activity at all (Table 1). Modifications of the  $\gamma$ -lactam core of lactacystin mitigate its inhibitory effect, but modifications of the *N*-acetylcysteine moiety do not. Although not ruling out alternative hypotheses, these results make the proteasome the likely candidate for the cellular target of lactacystin (23).

Rock *et al.* (24) used protease inhibitors to study the role of the proteasome in the degradation of various proteins. The peptide aldehyde inhibitors used in these studies were also shown to potentially inhibit the cysteine proteases calpain and cathepsin B. On the other hand, neither lactacystin nor the related  $\beta$ -lactone (both at 100  $\mu$ M) had a detectable effect on these or any other protease tested, including the serine proteases chymotrypsin and trypsin and the cysteine protease papain (3), even after more than 48 hours of exposure.

We next turned our attention to the issue of which residues of the primary lactacystin-binding protein are modified by lactacystin. On the basis of our kinetic studies, we surmised that modification of the primary lactacystin-binding protein, and not the secondary lactacystin-binding protein, was likely to be responsible for inhibition of at least the chymotrypsin-like and trypsin-like activities. These activities are inhibited by lactacystin and the  $\beta$ -lactone in a time frame where only a trace amount of modification of the secondary lactacystin-binding protein occurs.

The primary lactacystin-binding protein, labeled with [<sup>3</sup>H]lactacystin of low specific activity, was isolated from purified 20S proteasome by C4 rpHPLC and digested with trypsin (25). The tryptic fragments were then separated by narrowbore C18 rpHPLC. Two of the peaks contained radiolabel, and these were sequenced. The first had the sequence DAYSGGSVSLY (sequence 4 in Fig. 4A). On the basis of homology to subunit X/MB1, this fragment was expected to be internal, and the lack of sequence COOH-terminal to the tyrosine was thus unanticipated. The premature termination could have occurred for reasons unrelated to lactacystin, but it is possible

that the subsequent residue was modified. If this is the case, then the modified residue may be histidine, a potential catalytic base, which occurs at the corresponding position in human subunits X/MB1, LMP7, and their homologs in other organisms.

A stronger argument can be made for the identity of the modified residue in the second labeled fragment. The first cycle of Edman degradation did not produce an identifiable phenylthiohydantoin (PTH)-amino acid derivative, and subsequent cycles produced the sequence TTLAFK (underlined in sequence 1 in Fig. 4A), which is identical to residues 2 to 7 of the unmodified, undigested protein. From direct NH<sub>2</sub>-terminal sequencing of unlabeled protein, we found that the first residue is threonine, and the failure of this residue to appear as a standard PTH-amino acid derivative after reaction of the proteasome with lactacystin suggests that it is the modified residue. The mass spectrum (matrix-assisted laser desorption time-of-flight mass spectrometry, without internal calibrant) of the fragment contained a peak at *m/z* 992, which agrees well with the calculated value of 994 for the

NH<sub>2</sub>-terminal heptapeptide acylated by lactacystin. Whereas the primary lactacystin-binding protein contains an NH<sub>2</sub>-terminal TTT, proteasome chain  $\alpha$ , the secondary lactacystin-binding protein, contains the NH<sub>2</sub>-terminal sequence TTI (Fig. 4B); however, in this case, we found no indication that either threonine was modified from sequencing of this subunit isolated from lactacystin-treated 20S proteasome.

Threonine repeats are found at the mature, proteolytically processed NH<sub>2</sub>-termini of many proteasome subunits. Direct NH<sub>2</sub>-terminal sequencing of the archaeobacterial proteasome has revealed a threonine triad at the NH<sub>2</sub>-terminus (13). In the case of human LMP7 (26) and human subunit X/MB1 (10), an NH<sub>2</sub>-terminal TTT in the mature protein is suspected. The *S. cerevisiae* protein Pre2 also contains this sequence (27), although the NH<sub>2</sub>-terminus of the mature protein has not been established. Direct NH<sub>2</sub>-terminal sequencing of proteasome subunit  $\delta$  and the proteasome  $\alpha$  chain (6, 7), as well as sequencing of the MHC-encoded proteasome subunit LMP2 (28), has shown that the NH<sub>2</sub>-termini of the

**Table 1.** Kinetics of inhibition of the peptidase activities of purified 20S proteasome by lactacystin and analogs of lactacystin. Biological activity of compound refers to the ability of the compound to induce neurite outgrowth in Neuro-2a mouse neuroblastoma cells and to inhibit cell cycle progression in MG-63 human osteosarcoma cells (2). Experiments were performed as follows: Purified 20S proteasome (~5 ng/ $\mu$ l) (4) in 10 mM tris-HCl and 1 mM EDTA (pH 7.5) was incubated at 25°C in the presence of lactacystin or lactacystin analogs [dimethyl sulfoxide or CH<sub>3</sub>OH cosolvent not exceeding 5% (v/v)]. Aliquots for fluorescence assay were removed at various times after the addition of compound and diluted in 10 mM tris-HCl and 1 mM EDTA (pH 7.5) containing fluorogenic peptide substrates (100  $\mu$ M final concentration). Suc-LLVY-AMC, Cbz-GGR- $\beta$ NA, and Cbz-LLE- $\beta$ NA (AMC = 7-amido-4-methylcoumarin;  $\beta$ NA =  $\beta$ -naphthylamide Suc = succinyl, cbz = carbobenzyloxy) were used to assay the chymotrypsin-like, trypsin-like, and peptidylglutamyl-peptide hydrolyzing (PGPH) activities, respectively. Fluorescence excitation/emission wavelengths were 460 nm/380 nm for AMC and 410 nm/335 nm for  $\beta$ NA. The fluorescence assays were conducted at 25°C, and each experiment was performed at least three times. The  $k_{\text{assoc}}$  values represent mean  $\pm$  standard deviation. Association of an irreversible inhibitor with an enzyme is often depicted in two steps,  $E + I \rightleftharpoons E \cdot I \rightarrow E-I$ , where E-I is the stable enzyme-inhibitor complex. If the rate constants for the reversible first step are  $k_1$  and  $k_{-1}$ , and the rate constant for the irreversible second step is  $k_2$ , then the second-order rate constant  $k_{\text{assoc}}$  is given by  $k_1 k_2 / k_{-1}$ . This value may be calculated without determining the microscopic rate constants from the pseudo-first order association rate constant  $k_{\text{obs}}$ , which is in turn derived from plots of  $\ln(v_t/v_0)$  versus time (where  $v_t$  = the velocity at time  $t$  and  $v_0$  = velocity at time zero).  $k_{\text{assoc}}$  is equal to  $k_{\text{obs}}/[I]$ . Blanks indicate not applicable.

Compound (concentration)	$k_{\text{assoc}} = k_{\text{obs}}/[I]$ ( $M^{-1} s^{-1}$ )		
	Chymotrypsin-like activity	Trypsin-like activity	PGPH activity
<i>Biologically active compounds</i>			
Lactacystin (10 $\mu$ M)	194 $\pm$ 15	10.1 $\pm$ 1.8	4.2 $\pm$ 0.6
Lactacystin (100 $\mu$ M)	3059 $\pm$ 478		
$\beta$ -Lactone (1 $\mu$ M)		208 $\pm$ 21	59 $\pm$ 17
$\beta$ -Lactone (5 $\mu$ M)			
$\beta$ -Lactone (50 $\mu$ M)			
Lactacystin amide (12.5 $\mu$ M)	362 $\pm$ 40		
2'-Phenyllactacystin (12.5 $\mu$ M)	179 $\pm$ 19		
<i>Biologically inactive compounds</i>			
Dihydroxy acid (100 $\mu$ M)	No inhibition	No inhibition	No inhibition
6-Deoxylactacystin (12.5 $\mu$ M)	No inhibition		
(6 <i>R</i> ,7 <i>S</i> )Lactacystin (6-epi,7-epi) (12.5 $\mu$ M)	No inhibition		
Des(hydroxyisobutyl)lactacystin (12.5 $\mu$ M)	No inhibition		

processed forms of these proteins also begin with TTL. The widespread occurrence of the NH<sub>2</sub>-terminal threonine and the apparent modification of this residue on the primary lactacystin-binding protein by lactacystin suggest that NH<sub>2</sub>-terminal threonine residues may play an important catalytic role in these proteasome subunits. A possibility is that the side chain hydroxyl of the NH<sub>2</sub>-terminal threonine of proteasome subunit X/MB1 may be the nucleophile that attacks the amide carbonyl of peptide substrates, and the  $\alpha$ -amino group might act as a base to activate the threonine side chain hydroxyl. Duggleby *et al.* (29) suggested an analogous catalytic role for the NH<sub>2</sub>-terminal serine of penicillin acylase and postulated that a bridging water molecule might be involved in proton transfer. While this manuscript was in review, we learned that an x-ray crystal structure of the archaeobacterial proteasome has been solved to 3.4 Å resolution; the structure of this proteasome with a bound peptide aldehyde inhibitor, as well as mutagenesis studies, suggest that the NH<sub>2</sub>-terminal threonine of the mature  $\beta$  subunit contains the active site nucleophile (30), consistent with our finding that lactacystin modifies the NH<sub>2</sub>-terminal threonine of a related subunit in the eukaryotic proteasome.

Both lactacystin and the related  $\beta$ -lactone inhibit multiple peptidase activities of the proteasome and yet appear to modify predominantly one type of proteasome subunit, subunit X/MB1. Because the inhibition of the chymotrypsin-like and trypsin-like activities appears to be irreversible, covalent modification of subunit X/MB1 may be responsible for the inhibition of these activities. One explanation for such dual inhibition could be that formation of the lactacystin-protein adduct at one site causes a change in conformation that is transmitted to the different types of active sites. However, in this case, one would expect the kinetics of inhibition to be the same for the two activities. A more reasonable explanation is that subunit X/MB1 may be a component of both the chymotrypsin-like and trypsin-like active sites. One possibility is that subunit X/MB1 contains two residues modified by lactacystin, one of which is an active site nucleophile and the other of which forms part of a second active site at an interface with another subunit; for instance, the NH<sub>2</sub>-terminal threonine may be an active site nucleophile, and the second putative lactacystin-modified residue could be a base that activates an active site nucleophile on another subunit. Alternatively, subunit X/MB1 may contain two active site nucleophiles, each of which is associated with a separate type of active site. Another possibility is that

subunit X/MB1, present in multiple copies per proteasome particle, may possess only one active site nucleophile that participates in both activities; the active sites would form at an interface between a common region of subunit X/MB1 and other variable specificity-determining subunits in different locations and microenvironments in the proteasome particle.

Lactacystin is the most selective proteasome inhibitor presently known and thus may be a useful reagent for examining the role of the proteasome in proteolytic processes in the cell. It binds primarily to subunit X/MB1 and yet inhibits multiple proteasome activities. This implies that this subunit may play an important catalytic role in the proteasome and raises interesting questions about the proteasome's organization. Furthermore, the discovery that lactacystin modifies the highly conserved NH<sub>2</sub>-terminal threonine residue of subunit X/MB1, a possible active site nucleophile, may serve as a starting point for the elucidation of the detailed mechanism of proteolysis and for the construction of dominant-negative mutants of the proteasome.

#### REFERENCES AND NOTES

1. S. Omura *et al.*, *J. Antibiot.* **44**, 113 (1991); S. Omura *et al.*, *ibid.*, p. 117.
2. G. Fenteany *et al.*, *Proc. Natl. Acad. Sci. U.S.A.* **91**, 3358 (1994).
3. G. Fenteany *et al.*, data not shown.
4. The 20S proteasome was purified to homogeneity from bovine brain as follows (all operations were performed at 4°C except as noted, and all buffers contained 5 mM  $\beta$ -mercaptoethanol; pH was measured at 22°C). Fresh bovine brain (2 kg) was minced, frozen in liquid nitrogen, ground to a fine powder in a blender, and suspended in 6 liters of homogenization buffer [18.25 mM K<sub>2</sub>HPO<sub>4</sub>, 6.75 mM KH<sub>2</sub>PO<sub>4</sub>, 0.27 M sucrose, 2 mM EDTA, 2 mM EGTA, 25 mM NaF, 5 mM Na<sub>4</sub>P<sub>2</sub>O<sub>7</sub> (pH 7.7), and 5  $\mu$ g/ml each of leupeptin and pepstatin A]. The suspension was homogenized for an additional 2 min in the blender and then clarified by centrifugation in two stages (5000g, 15 min; 10,000g, 20 min). The material that precipitated from the homogenate between 50 and 60% saturation in ammonium sulfate contained lactacystin-binding activity, and this material was suspended in and dialyzed against 20 mM 2-[N-morpholino]ethane sulfonic acid-NaOH (pH 5.7). The dialyzed solution was then loaded onto a 2.5 cm by 25 cm column of SP-Sepharose FF (Pharmacia) equilibrated with the same buffer, and a 500-ml gradient of 0 to 300 mM NaCl was applied. Fractions binding lactacystin were pooled, adjusted with tris buffer to pH 8, diluted, and chromatographed on a 1.6 cm by 8 cm column of Q-Sepharose FF (Pharmacia) with a buffer of 20 mM tris-HCl (pH 8.0) and a 120-ml gradient from 0 to 500 mM NaCl. Appropriate fractions were pooled, concentrated by ultrafiltration, and chromatographed on a Superose 6 HR 10/30 gel filtration column (Pharmacia) with a buffer of 10 mM tris-HCl and 1 mM EDTA (pH 7.5) at a flow rate of 0.5 ml/min (the gel filtration standards used were dextran blue, thyroglobulin, apoferritin,  $\beta$ -amylase, alcohol dehydrogenase, bovine serum albumin, and carbonic anhydrase).
5. The ratio of radioactivity incorporated into the first eluted peak versus the second peak varied with the length of incubation and the ligand; the rate of radiolabeling of the first peak was always much slower than of the second. A 24-hour reaction resulted in

19% as much radioactivity incorporated into the first peak as into the second with [<sup>3</sup>H] $\beta$ -lactone (Fig. 3) and 32% with [<sup>3</sup>H]lactacystin (3). The apparent selectivity runs opposite to the relative chemical reactivity of the two compounds, which suggests that the N-acetylcysteine moiety of lactacystin may facilitate the interaction with the protein in the first peak, the secondary lactacystin-binding protein, or that the free  $\beta$ -lactone in solution may be unstable with long incubation.

6. L. W. Lee, *et al.*, *Biochim. Biophys. Acta* **1037**, 178 (1990).
7. K. Lilley, M. Davison, A. J. Rivett, *FEBS Lett.* **262**, 327 (1990).
8. P. Haffter and T. D. Fox, *Nucleic Acids Res.* **19**, 5075 (1991).
9. K. Akiyama *et al.*, *Science* **265**, 1231 (1994).
10. M. Belich, R. J. Glynn, G. Senger, D. Sheer, J. Trowsdale, *Curr. Biol.* **4**, 769 (1994).
11. M. Orlowski, *Biochemistry* **29**, 10289 (1990); K. Tanaka, T. Tamura, T. Yoshimura, A. Ichihara, *New Biol.* **4**, 173 (1992).
12. B. Dahlmann *et al.*, *FEBS Lett.* **251**, 125 (1989).
13. P. Zwickle *et al.*, *Biochemistry* **31**, 964 (1992).
14. A. Grziwa, W. Baumeister, B. Dahlmann, F. Kopp, *FEBS Lett.* **290**, 186 (1991); G. Pühler *et al.*, *EMBO J.* **11**, 1607 (1992).
15. M. Rechsteiner, L. Hoffman, W. Dubiel, *J. Biol. Chem.* **268**, 6065 (1993); J.-M. Peters, *Trends Biochem. Sci.* **19**, 377 (1994).
16. The reversibility of the inhibition was assessed by measuring residual peptidase activity after removal of the inhibitor by extensive serial dilution and ultrafiltration. This procedure did not lead to any recovery of the trypsin-like and chymotrypsin-like activities, implying a very low off rate of inhibitor from enzyme, whereas control samples not treated with inhibitor remained active toward the peptide substrates over a period of days (3). In the case of the PGPH activity, removal of the inhibitor was accompanied by a return of the catalytic activity. The inhibition of the PGPH activity could be due to noncovalent association of lactacystin with the PGPH site or covalent association with turnover of the enzyme-lactacystin complex.
17. M. Rechsteiner, *Cell* **66**, 615 (1991); D. Finley and V. Chau, *Ann. Rev. Cell Biol.* **7**, 25 (1991); A. Hershko and A. Ciechanover, *Annu. Rev. Biochem.* **61**, 761 (1992); A. Ciechanover, *Cell* **79**, 13 (1994).
18. A. L. Goldberg and K. L. Rock, *Nature* **357**, 375 (1992).
19. A. W. Murray, M. J. Solomon, M. W. Kirschner, *ibid.* **339**, 280 (1989).
20. M. Glotzer, A. W. Murray, M. W. Kirschner, *ibid.* **349**, 132 (1991); A. Hershko, D. Ganoh, J. Pehrson, R. E. Palazzo, L. H. Cohen, *J. Biol. Chem.* **266**, 16376 (1991).
21. V. J. Palombella, O. J. Rando, A. L. Goldberg, T. Maniatis, *Cell* **78**, 773 (1994).
22. J. Hagler, O. J. Rando, G. Fenteany, S. L. Schreiber, T. Maniatis, unpublished results.
23. The tripeptide aldehyde benzyloxycarbonyl-Leu-Leu-leucinal has been shown to induce neurite outgrowth in PC12 rat pheochromocytoma cells, and the 20S proteasome was suggested as a target of the compound [Tsubuki *et al.*, *Biochem. Biophys. Res. Commun.* **196**, 1195 (1993)]. However, neurite outgrowth in response to this tripeptide aldehyde could also be due to inhibition of another protease. Although lactacystin inhibits growth of PC12 cells, it does not appear to induce neurite outgrowth in this cell line (2).
24. K. L. Rock *et al.*, *Cell* **78**, 761 (1994).
25. Purified 20S proteasome (~0.1  $\mu$ g/ $\mu$ l) (3) was incubated for 24 hours at room temperature with 10  $\mu$ M lactacystin in 10 mM tris-HCl and 1 mM EDTA (pH 7.5). The solution was then diluted 1:10 with 20% aqueous acetonitrile containing 0.1% trifluoroacetic acid (TFA) and allowed to stand at room temperature for 5 min. The rpHPLC was performed as described in the legend of Fig. 3. Peaks were collected on the basis of absorbance at 210 and 280 nm, and protein from repeated injections was pooled, lyophilized, and subjected to Edman degradation on an Applied Biosystems 477A or Hewlett Packard G1005 protein sequencer after

- tryptic digestion and Vydac narrowbore C18 (300 Å, 2.1 mm by 150 mm) rpHPLC separation of tryptic fragments. Matrix-assisted laser desorption time-of-flight (MALDI-TOF) mass spectrometry was performed on a Finnigan LaserMat 2000. The putative lactacystin-modified residue on the primary lactacystin-binding protein was identified by adding a small amount of subunit X/MB1 isolated from [<sup>3</sup>H]lactacystin-treated proteasome to a sample that had been treated with unlabeled lactacystin, and then isolating and sequencing radioactive tryptic fragments.
26. K. Früh *et al.*, *J. Biol. Chem.* **267**, 22131 (1992).
  27. W. Heinemeyer, A. Gruhler, V. Mohrle, Y. Mahe, D. H. Wolf, *ibid.* **268**, 5115 (1993).
  28. C. K. Martinez and J. J. Monaco, *Nature* **353**, 664 (1991).
  29. H. J. Duggleby *et al.*, *ibid.* **373**, 264 (1995).
  30. J. Löwe, D. Stock, B. Jap, W. Baumeister, R. Huber,

*Science* **268**, 533 (1995); E. Seemüller *et al.*, *ibid.*, p. 579.

31. D. B. Dess and J. C. Martin, *J. Am. Chem. Soc.* **113**, 7277 (1991).
32. We thank V. Bailey, R. Robinson, D. Lizotte, J. Neveu, and E. Spooner of the Harvard Microchemistry Facility for protein sequencing and mass spectrometry. This research was funded in part by grants from the National Institute of General Medical Sciences to E.J.C. and S.L.S. G.F. was supported by a National Defense Science and Engineering Graduate Fellowship, and R.F.S. was supported by a fellowship from the Merck, Sharp & Dohme Research Laboratories Academic Development Program. S.L.S. is a Howard Hughes Medical Institute Investigator.

9 March 1995; accepted 29 March 1995

## Translational Suppression by Trinucleotide Repeat Expansion at *FMR1*

Yue Feng, Fuping Zhang, Laurie K. Lokey, Jane L. Chastain, Lisa Lakkis, Derek Eberhart, Stephen T. Warren\*

Fragile X syndrome is the result of the unstable expansion of a trinucleotide repeat in the 5'-untranslated region of the *FMR1* gene. Fibroblast subclones from a mildly affected patient, each containing stable *FMR1* alleles with 57 to 285 CGG repeats, were shown to exhibit normal steady-state levels of *FMR1* messenger RNA. However, FMR protein was markedly diminished from transcript with more than 200 repeats. Such transcripts were associated with stalled 40S ribosomal subunits. These results suggest that a structural RNA transition beyond 200 repeats impedes the linear 40S migration along the 5'-untranslated region. This results in translational inhibition by trinucleotide repeat expansion.

Fragile X syndrome is a frequent cause of mental retardation that is inherited as an X-linked dominant with reduced penetrance (1). The mutational change in nearly all affected patients is the unstable expansion of a CGG trinucleotide repeat in the 5'-untranslated region of the *FMR1* gene (2-4). This repeat is normally polymorphic in length and content, exhibiting a mode of 30 cryptic repeats in the normal population, but the triplet is found in excess of ~230 repeats in affected patients, often approaching 1000 copies (5, 6). Male and most female carriers have an *FMR1* premutation with an intermediate number of repeats, between about 60 and 200 triplets. In most penetrant males with full-mutation alleles containing >230 CGG repeats, the *FMR1* gene is abnormally methylated and transcriptionally suppressed (7-10). The absence of the encoded protein, FMRP, a selective RNA-binding protein, is responsible for the clinical phenotype (11). About 15% of male patients do express *FMR1* mRNA and are termed mosaics, because they display a complex pattern of repeat size

variation as well as incomplete methylation (3, 7, 12). A range of phenotypes from normal to penetrant, including severe mental retardation, has been found in this group. However, no clear correlation has emerged between the degree of hypomethylation, the extent of *FMR1* expression, and clinical involvement (12, 13). It has thus remained unclear if *FMR1* transcription is the sole determinant of penetrance or if other influences, such as translational suppression by lengthy CGG repeats in the *FMR1* transcript, affect FMRP levels.

A mildly affected 19-month-old male with near-normal cognitive and developmental abilities and slight physical features suggesting fragile X syndrome was studied (14). Polymerase chain reaction (PCR) analysis of the *FMR1* CGG repeat (Fig. 1A) showed a broad smear ranging in size from about 100 to 300 repeats in the patient (III-2), with a maternal premutation allele of ~70 repeats (II-3) and grandmaternal premutation allele of ~60 repeats (I-2), exhibiting the typical repeat instability found in fragile X syndrome kindred. We confirmed the PCR analysis by Southern (DNA) blot analysis (Fig. 1B) and demonstrated that the patient's gene was predominantly unmethylated (>90% by densitometry) by exhibiting

cleavage with a methyl-sensitive enzyme, either Bss HII or Eag I. The broad 3.6-kb band, observed in both lymphocytes and fibroblasts of the patient, reflected a mean repeat length of ~290 triplets in an unmethylated state. Thus, this patient was atypical of most fragile X patients and carriers, because the repeat length was larger than that observed in nonpenetrant carriers, but in contrast to affected patients, including most mosaic males, nearly all cells exhibited the normal, unmethylated status of the *FMR1* gene.

Normal levels of *FMR1* mRNA were detected in the patient's lymphocytes and fibroblasts. Reverse transcriptase PCR across the repeat demonstrated concordance of repeat lengths between DNA and RNA. However, a protein immunoblot with a monoclonal antibody against FMRP (15) revealed only ~30% of normal FMRP levels relative to the control,  $\beta$ -tubulin. Instead of a general reduction in FMRP levels, immunofluorescent staining of FMRP in the patient's fibroblasts showed a mosaic pattern of variable reactivity (Fig. 2). This was in contrast to the more consistently positive cells of a normal male or the uniformly negative cells of a typically affected male, suggesting a FMRP level intrinsic to each cell of the patient.

To more fully evaluate this finding, we isolated individual fibroblast clones from low-density cultures. Seven clones were identified for further study by PCR amplification of the *FMR1* CGG repeat from DNA samples derived from independent fibroblast colonies. The clones displayed discrete repeat lengths of 57, 168, 182, 207, 266, 285, and 285 triplets, which spans the range of mosaicism in the patient's fibroblasts (Fig. 3A). Each clonal isolate contained hypomethylated *FMR1* alleles, which maintained a stable repeat length upon culture expansion. Steady-state RNA levels were evaluated in each clonal population by ribonuclease (RNase) protection of *FMR1* mRNA hybridized with <sup>32</sup>P-labeled antisense RNA and normalized to  $\gamma$ -actin signal as control. No significant differences in steady-state levels of *FMR1* mRNA were observed between or among the normal controls (30 and 32 repeats) and the patient's clonal cell populations (57 to 285 repeats) (Fig. 3B). Densitometric quantitation of *FMR1* signal (16) showed  $101 \pm 21.4$  units for normals ( $n = 14$ ) versus  $124 \pm 29$  units for the patient's clones ( $n = 7$ ). A typical fully penetrant male sample, with about 962 methylated repeats, showed no *FMR1* transcript, as expected (Fig. 3B, lane 9). These data therefore confirm and extend our previous demonstration of quantitatively similar levels of *FMR1* gene transcription between normal and premutation alleles of <100 CGG repeats (16).

Howard Hughes Medical Institute and Departments of Biochemistry and Pediatrics, Emory University School of Medicine, Atlanta, GA 30322, USA.

\*To whom correspondence should be addressed. E-mail: swarren@bimcore.emory.edu.